

Cobalt Carbonyl Complexes with Bridging Diphosphine Ligands

Hameed A. Mirza, Jagadese J. Vittal, and Richard J. Puddephatt*

Department of Chemistry, University of Western Ontario, London, Ontario, Canada N6A 5B7

Christopher S. Frampton and Ljubica Manojlović-Muir

Department of Chemistry, University of Glasgow, Glasgow G12 8QQ, Scotland, U.K.

Wenjia Xia and Ross H. Hill

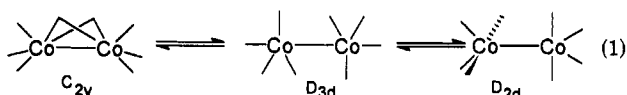
Department of Chemistry, Simon Fraser University, Burnaby, British Columbia, Canada V5A 1S6

Received December 2, 1992

Reduction of cobalt(II) chloride by Na[BH₄] in the presence of CO and dmpm (=Me₂PCH₂-PMe₂) gave either [Co₂(CO)₂(μ-CO)₂(μ-dmpm)₂] (1a) or [Co₄(CO)₅(μ-CO)₃(μ-dmpm)₂] (6), depending on the reaction stoichiometry. Complex 1a, in solution is in equilibrium with its isomer [Co₂(CO)₄(μ-dmpm)₂] (2a), and the thermodynamic parameters for the reaction were determined by measuring the equilibrium constant as a function of temperature using FTIR. The activation energy for the isomerization was determined by variable-temperature NMR studies, which also indicated that 2a is weakly paramagnetic. Reaction of 1a with iodine or [Cu(NCMe)₄]⁺ gave [Co₂(μ-I)(μ-CO)(CO)₂(μ-dmpm)₂]⁺ (7) and [Co₄Cu₃(CO)₈(μ-dmpm)₂]⁺ (8), respectively. The molecular structures of 6 and 8 were characterized by X-ray diffraction (6, orthorhombic, P2₁2₁2₁, a = 14.953(2) Å, b = 11.386(1) Å, c = 16.836(1) Å, Z = 4, R = 0.038; 8, monoclinic, P2₁/c, a = 10.767(2) Å, b = 20.092(2) Å, c = 22.370(3) Å, β = 92.13°, Z = 4, R = 0.076). Complex 6 contains an irregular tetrahedral Co₄ cluster with two edges bridged by dmpm ligands and one face edge-bridged by carbonyl groups. The Co-Co bond lengths are 2.426(1)-2.541(2) Å. The cluster 8 contains a central copper atom with approximately square-planar stereochemistry, which is apparently unique in copper clusters.

Introduction

Dicobalt octacarbonyl, [Co₂(CO)₈], was important in the development of carbonyl chemistry and homogeneous catalysis, and so it has been much studied.^{1,2} In the solid state, the structure is of C_{2v} symmetry with two bridging carbonyls,³ but in solution two nonbridged forms with D_{3d} and D_{2d} symmetry also exist (eq 1).⁴ However, the



interconversions are too rapid even at -150 °C to allow a study of the dynamics by ¹³C NMR spectroscopy. Many phosphine derivatives of [Co₂(CO)₈] are known, most being formed by phosphine for carbonyl substitution reactions.⁵⁻¹³

Among these are [Co₂(CO)₄(μ-CO)₂(μ-PP)] (PP = dppm, dmpm) and the isomers [Co₂(CO)₂(μ-CO)₂(μ-PP)₂] and [Co₂(CO)₄(μ-PP)₂] (PP = dppm = Ph₂PCH₂PPh₂). These complexes are also fluxional.

Thermolysis of [Co₂(CO)₈] yields the cluster [Co₄(CO)₁₂], which is formulated as [Co₄(CO)₉(μ-CO)₃] with approximate C_{3v} symmetry and which is also fluxional.¹⁴⁻¹⁷ It has been shown that up to four CO groups in [Co₄(CO)₁₂] can be substituted with monodentate phosphines to give complexes of the type [Co₄(CO)_{12-n}L_n]^{7,18} with n = 1-4 and with bidentate phosphine ligands to give [Co₄(CO)_{12-2n}(PP)_n].^{5,7,19}

This paper describes related dinuclear and tetranuclear cobalt carbonyl complexes, with bridging Me₂PCH₂PMe₂ (=dmpm) ligands, which are synthesized by direct re-

(9) de Leeuw, G.; Field, J. S.; Haines, R. J. *J. Organomet. Chem.* 1989, 359, 245.

(10) Brown, G. M.; Finholt, J. E.; King, R. B.; Bibber, J. W. *Inorg. Chem.* 1982, 21, 2139.

(11) Laneman, S. A.; Fronczek, F. R.; Stanley, G. G. *Inorg. Chem.* 1989, 28, 1207.

(12) Newton, M. G.; King, R. B.; Chang, M.; Pantaleo, N. S.; Gimeno, J. *J. Chem. Soc., Chem. Commun.* 1977, 531.

(13) Chai, L. S.; Cullen, W. R. *Inorg. Chem.* 1975, 14, 482.

(14) Sweany, R. L.; Brown, T. L. *Inorg. Chem.* 1977, 16, 415.

(15) Carré, F. H.; Cotton, F. A.; Frenz, B. A. *Inorg. Chem.* 1976, 15, 380.

(16) Johnson, B. F. G.; Benfield, R. E. *J. Chem. Soc., Dalton Trans.* 1978, 1554.

(17) (a) Aime, S.; Osella, D.; Milone, L.; Hawkes, G. E.; Randall, E. W. *J. Am. Chem. Soc.* 1981, 103, 5920. (b) Hanson, B. E.; Lisic, E. C. *Inorg. Chem.* 1986, 25, 715. (c) Aime, S.; Botta, M.; Gobetto, R.; Hanson, B. E. *Inorg. Chem.* 1989, 28, 1196. (d) Heaton, B. T.; Sabounchei, J.; Kernaghan, S.; Nakayama, H.; Eguchi, T.; Takeda, S.; Nakamura, N.; Chihara, H. *Bull. Chem. Soc. Jpn.* 1990, 63, 3019. (e) *J. Organomet. Chem.* 1992, 428, 207.

(18) Darensbourg, D. J.; Incorvia, M. J. *Inorg. Chem.* 1981, 20, 1911.

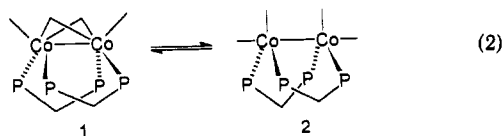
(19) King, R. B.; Gimeno, J.; Lotz, T. J. *Inorg. Chem.* 1978, 17, 2401.

(1) Mond, L.; Hirzt, H.; Cowap, M. D. *J. Chem. Soc.* 1910, 798.
 (2) Heck, R. F. *Organotransition Metal Chemistry*; Academic Press: Toronto, 1974.
 (3) Summer, G. G.; Klug, H. P.; Alexander, L. E. *Acta Crystallogr.* 1964, 17, 732.
 (4) (a) Bor, G.; Noack, K. *J. Organomet. Chem.* 1974, 64, 367. (b) Bor, G.; Dieter, U. K.; Noack, K. *J. Chem. Soc., Chem. Commun.* 1976, 914.
 (c) Onaha, S.; Shriver, D. F. *Inorg. Chem.* 1976, 15, 915.
 (5) Lisic, E. C.; Hanson, B. E. *Inorg. Chem.* 1986, 25, 812.
 (6) (a) Attali, S.; Poilblanc, R. *Inorg. Chim. Acta* 1972, 6, 475. (b) Mantasti, E.; Pelizzetti, E.; Rossetti, R.; Stanghellini, P. L. *Inorg. Chim. Acta* 1977, 25, 7.
 (7) Wilkinson, G., Ed. *Comprehensive Organometallic Chemistry*; Pergamon Press: Toronto, 1982; Vol. 5.
 (8) (a) Harrison, W.; Trotter, J. *J. Chem. Soc. A* 1971, 1607. (b) Cullen, W. R.; Crow, J.; Harrison, W.; Trotter, J. *J. Am. Chem. Soc.* 1970, 92, 6339. (c) Thornhill, D. J.; Manning, A. R. *J. Chem. Soc., Dalton Trans.* 1973, 2086. (d) Fukumoto, T.; Matsumura, Y.; Okawara, R. *J. Organomet. Chem.* 1978, 69, 437.

duction of cobalt(II) halides in the presence of CO and dmpm. Some chemistry of $[\text{Co}_2(\text{CO})_2(\mu\text{-CO})_2(\mu\text{-dmpm})_2]$, including the formation of an unusual Co_4Cu_3 cluster, is also described. Preliminary accounts of parts of this work have been published.^{20,21}

Synthesis and Characterization of $[\text{Co}_2(\text{CO})_2(\mu\text{-CO})_2(\mu\text{-dmpm})_2]$ (1)

Reduction of cobalt(II) chloride by NaBH_4 in the presence of excess dmpm and CO gave the yellow-orange product $[\text{Co}_2(\text{CO})_2(\mu\text{-CO})_2(\mu\text{-dmpm})_2]$ (1a). The solid-state IR spectrum of 1a contained bands due to both terminal and bridging carbonyl groups and was very similar to that of $[\text{Co}_2(\text{CO})_2(\mu\text{-CO})_2(\mu\text{-dppm})_2]$ (1b), whose structure has been determined by X-ray diffraction.²² However, in CH_2Cl_2 solution at room temperature, the bridging carbonyl band was absent and it is clear that isomerization to an isomer with only terminal carbonyls, $[\text{Co}_2(\text{CO})_4(\mu\text{-dmpm})_2]$ (2a), is responsible (eq 2). The solution IR



spectrum at -90°C contained both bridging and terminal CO groups, indicating that the equilibrium of eq 2 lies to the left at low temperature and the right at higher temperature.

The thermodynamics of the equilibrium of eq 2 in dichloromethane solution were studied by variable-temperature solution FTIR spectroscopy (Figure 1). The observation of isosbestic points indicates a simple equilibrium between two isomers. Equilibrium constants were determined from these spectra over the temperature range 190–301 K, and a plot of $\ln K$ vs $1/T$ resulted in a good linear fit (Figure 1). The thermodynamic data for 1 and 2 (PP = dmpm, dppm) and the parent $[\text{Co}_2(\text{CO})_8]$ are presented in Table I. For the diphosphine-bridged complexes, the enthalpy term strongly favors the bridged form (1), while the entropy term strongly favors the unbridged form (2) in each case. The effect is much greater than for the parent $[\text{Co}_2(\text{CO})_8]$ (Table I). An attempt was made to determine the equilibrium constants independently by variable-temperature UV-visible absorption spectroscopy. Complex 2a absorbs more strongly than 1a over the region 520–700 nm, but the bandwidths appear to be temperature dependent and so quantitative data could not be obtained.

The ^{31}P NMR spectrum of the equilibrium mixture of 1a and 2a in acetone- d_6 at room temperature, where 2a is predominant, contained a single broad resonance at δ 14.1. At -90°C , where 1a is predominant, the spectrum contained a sharp singlet resonance at δ 33.2, assigned to 1a, and a barely resolved, extremely broad, weak resonance at δ 20.5, assigned to 2a. At intermediate temperatures (0 to -20°C) the ^{31}P NMR was very broad. It is therefore clear that the interconversion of 1a and 2a is fast at room

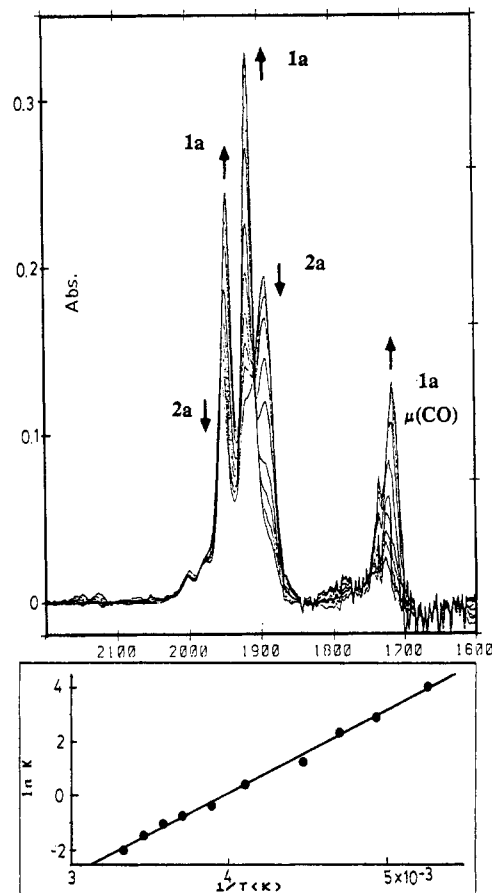


Figure 1. Variable-temperature FTIR spectra in the carbonyl region for the equilibrium mixture 1a/2a. The arrows indicate the growth or decay of peaks as the temperature is decreased, while at the bottom is the derived plot of $\ln K$ vs $1/T$.

Table I. Thermodynamic and Kinetic Data for the Equilibrium 1/2^a

complex	$\Delta H/\text{kJ mol}^{-1}$	$\Delta S/\text{J K}^{-1} \text{mol}^{-1}$	ratio 1:2		$\Delta G^\circ/\text{kJ mol}^{-1}$
			298 K	190 K	
$[\text{Co}_2(\text{CO})_8]$	+5.6	+21	44:56	74:26	27
1a/2a	+26.3(2.1)	+107(13)	9:91	98:2	47(1)
1b/2b	+22.1(1.5)	+102(8)	3:97	85:15	41.5(1)

^a Data in the case of $[\text{Co}_2(\text{CO})_8]$ are for solutions in pentane or hexane, while in the case of 1/2 data are for solutions in CH_2Cl_2 .

temperature such that only an average signal is observed but that separate signals are observed at low temperature. However, there must also be a very significant temperature dependence of the chemical shift of one or both isomers, since separate shifts of δ 33.2 and 20.5 cannot result in an average of δ 14.1. Spectra between -30 and -80°C were consistent with this assignment, but the signal assigned to -2a was always extremely broad, such that there remained some doubt. Therefore, the ^{31}P NMR spectra in CD_2Cl_2 of 1b/2b, both of which have been structurally characterized,²² were reinvestigated. The spectrum at 20 and -32°C each contained a singlet at δ 34.3 and 37.1, respectively, while at -52 and -72°C two singlets were observed at δ 41.9 (1b), 37.3 (2b) and 44.8 (1b), 37.7 (2b), respectively. There was further change of chemical shifts at -95°C , but no further splittings were observed. In the case of the 1b/2b equilibrium, both resonances were well resolved (Figure 2) and so the assignments are secure. The temperature dependence of the chemical shifts is significantly less than for 1a/2a, but the trend is the same. Of course, part of the change in average chemical shift is

(20) Elliot, D. J.; Mirza, H. A.; Puddephatt, R. J.; Holah, D. G.; Hughes, A. N.; Hill, R. H.; Xia, W. *Inorg. Chem.* 1989, 28, 3282.

(21) Mirza, H. A.; Vittal, J. J.; Puddephatt, R. J. *J. Chem. Soc., Chem. Commun.* 1991, 309.

(22) Elliot, D. J.; Holah, D. G.; Hughes, A. N.; Magnuson, V. R.; Moser, I. M.; Puddephatt, R. J. *Bull. Soc. Chim. Fr.* 1992, 129, 676.

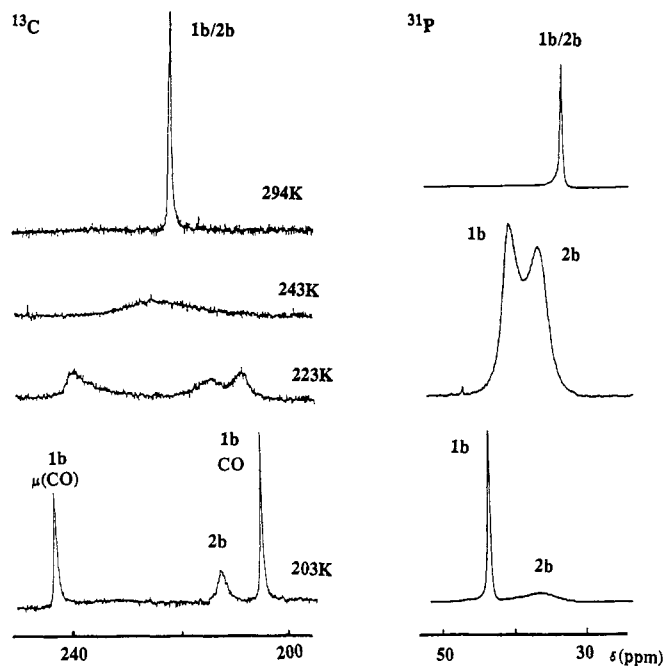


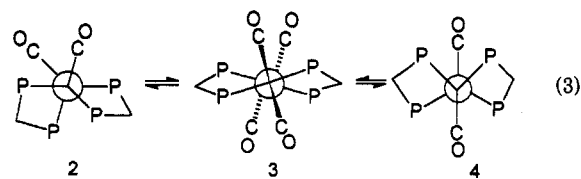
Figure 2. Variable-temperature ^{13}C NMR (75 MHz) and ^{31}P NMR (121 MHz) spectra for the mixture 1b/2b.

due to the strong temperature dependence of the equilibrium constant for eq 2. The 1b:2b ratios at 21, -32, -52, and -72 °C are 4:96, 22:78, 44:56, and 72:28, respectively. However, it is clear that the δ values of individual isomers decrease at higher temperatures and that the effect is stronger for the dmpm complexes 1a/2a.

The room-temperature ^1H NMR spectrum of 1a/2a in CD_2Cl_2 shows a broad resonance at δ 2.35 for the CH_2P_2 protons of the dmpm ligand and another resonance at δ 1.5 for the PMe protons. At -90 °C, the resonances due to $\text{CH}^a\text{H}^b\text{P}_2$ protons of 1a appeared as an AB pattern at δ 1.93 and 2.75 while a very weak peak at δ 2.19 was assigned to the CH_2P_2 protons of 2a. In addition, broad resonances at δ 1.50 and 1.34 (weak) were assigned to the Me_2P protons.

No carbonyl resonance was resolved in the room-temperature ^{13}C NMR spectrum of 1a/2a. However, at -82 °C two carbonyl resonances were observed at δ 203.5 and 265.5, assigned to the terminal and bridging carbonyls, respectively, of 1a. No resonance due to 2a was resolved. This could be due to the low abundance of 2a (only 2% at -82 °C), but at intermediate temperatures where the abundance is higher, based on the thermodynamic data of Table I, the resonance was still absent. For the dpmp analogs 1b/2b ^{13}C resonances were observed for both isomers, although that due to 2b was broad (Figure 2) and a coalesced signal was observed at room temperature.

It is interesting that the solid-state structure of $[\text{Co}_2(\text{CO})_4(\mu\text{-dpmp})_2]$ (2b) clearly indicates chemical inequivalence of the carbonyl groups occupying axial and equatorial sites on cobalt²² but only one carbonyl resonance was observed at low temperature. Moreover, the reaction shown in eq 2 for the equilibrium between 1 and 2 does not of itself lead to equivalence of carbonyl groups or the CH^aH^b protons of the unbridged form. This confirms that a second form of fluxionality with a much lower activation energy must occur within the nonbridged form 2. A reasonable mechanism for this fluxional process, which makes all carbonyls and CH_2P_2 protons equivalent, is illustrated by eq 3 (note that when only two carbonyls are



shown the other two are vertical to the plane of the paper). The structures are shown as Newman projections along the Co-Co bond. The reversible reaction $2 \rightleftharpoons 3$ is most reasonable, as structure 3 is analogous to the structure of the D_{2d} isomer of $[\text{Co}_2(\text{CO})_8]$ (eq 1). The formation of a third isomer (4) is possible but not necessary to explain the NMR data. A simpler interpretation of the NMR data, suggested by a reviewer, is that 3 is more stable than 2 in solution and that the equilibrium is between 1 and 3. A temperature-dependent equilibrium between 2 and 3 is inconsistent with the FTIR data discussed above; therefore, this interpretation requires 3 to be significantly more stable than 2 in solution over the whole temperature range studied. The problem with this interpretation is that 2 is the form that has been structurally characterized in the solid state.²²

The approximate activation energies ΔG^\ddagger for the equilibration between isomers was calculated by using the Eyring equation and are given in Table I. The activation energy for a given equilibration was constant, within the error bars given in Table I, over the temperature ranges for which coalescence of observable NMR resonances occurred. These temperature ranges were 233–275 or 213–243 K for 1a/2a or 1b/2b, respectively; hence, the entropy of activation is small. There is a clear correlation between the values of ΔH and ΔG^\ddagger for a given complex (Table I); in particular, the values of both parameters are much larger for 1/2 than for the corresponding isomers in $[\text{Co}_2(\text{CO})_8]$.

The strong dependence of $\delta(^{31}\text{P})$ of 1a/2a on temperature, the extreme broadness of the ^{31}P resonance of 2a, and the inability to detect the ^{13}C resonance of 2a were puzzling and suggested that 2a might be paramagnetic. It is known that the Co-Co distance in 2b (2.819(2) Å) is much longer than in 1b (2.44(3) Å),²² and this observation indicates a very weak Co-Co bond in 2b. Therefore, the magnetic susceptibility of complexes 1a/2a in solution was determined as a function of temperature by using Evans' method.²³ The results are given in Table II. The mixtures of 1a/2a are paramagnetic in solution, and the value of μ_{eff} increases with temperature as the proportion of 2a increases. The values of μ_{eff} at 201 and 298 K were 0.84 and 1.24 μ_B and correspond to 2a:1a ratios of 5:95 and 91:9, respectively (Table II). Considering that some temperature-independent paramagnetism is expected, the value of μ_{eff} at 298 K is clearly too low to indicate that 2a has two unpaired electrons, as expected for the diradical 5, but is consistent with an equilibrium between metal-metal-bonded and diradical forms 2a and 5; eq 4) or to a high-spin/low-spin equilibrium for 2a.²⁴ Similar solution paramagnetism has been observed in $[\text{Co}_2\text{H}(\mu\text{-H})_3(i\text{-Pr}_2\text{PCH}_2\text{CH}_2\text{CH}_2\text{P-}i\text{-Pr}_2)_2]$ and was attributed either to a

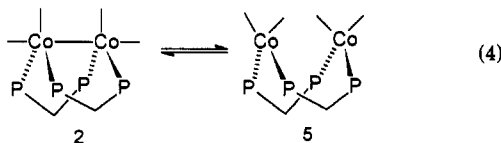
(23) (a) Evans, D. F. *J. Chem. Soc.* 1959, 2003. (b) Ostfeld, D.; Cohen, I. A. *J. Chem. Educ.* 1972, 49, 829. (c) Tiers, G. V. D. *J. Phys. Chem.* 1958, 62, 1151. (d) Washburn, E. W. *International Critical Tables*; McGraw-Hill: New York, 1929; Vol. III, p 27 and Vol. IV, p 361. (e) Figgis, B. N.; Lewis, J. In *Modern Coordination Chemistry*; Lewis, J. Wilkins, R. G., Eds.; Interscience: New York, 1960.

(24) (a) Baird, M. C. *Chem. Rev.* 1988, 88, 1217. (b) Fryzuk, M. D.; Ng, J. B.; Rettig, S. J.; Huffman, J. C.; Jonas, K. *Inorg. Chem.* 1991, 30, 2437.

Table II. Magnetic Moments (μ_B) of **1a/2a** in CD_2Cl_2 Solution as a Function of Temperature

	T/K						
	201	221	241	251	261	273	298
ratio ^a 1a:2a	95:5	81:19	56:44	44:56	32:68	22:78	9:91
μ_{eff}^b	0.84	0.98	1.10	1.14	1.19	1.26	1.24

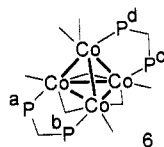
^a These values are estimated from the thermodynamic data obtained from FTIR studies (Table I). ^b This includes the diamagnetic correction; estimated error is $\pm 0.05 \mu_B$.



high-spin/low-spin equilibrium or to reversible dissociation to monomeric complexes.²⁴ It is not clear if the proposed paramagnetic complex might play a part in the fluxionality of **1a/2a**, but it is presumably responsible for the anomalous NMR properties of **2a** discussed earlier. Both the NMR data and magnetic properties were reproducible with carefully purified samples and so are unlikely to be caused by impurities of cobalt(II), while the FTIR data preclude reversible dissociation to mononuclear complexes. No EPR signal could be detected for **1a** in the solid state or for **1a/2a** in dichloromethane solution at room temperature or in a glass at liquid-nitrogen temperature. In the solid state, a mixture of **1b/2b** had $\mu_{eff} = 1.1 \mu_B$, while **1a** was diamagnetic.

Synthesis and Characterization of $[Co_4(CO)_5(\mu-CO)_3(\mu-dmpm)_2]$ (**6**)

Reduction of cobalt(II) chloride by $NaBH_4$ in the presence of a stoichiometric quantity of dmpm and excess CO gave the black product $[Co_4(CO)_5(\mu-CO)_3(\mu-dmpm)_2]$. The only difference from the reaction which gave $[Co_2(CO)_4(dmpm)_2]$ was the Co:dmpm ratio, which was ca. 1:1 and 1:3 in the synthesis of **6** and **1a**, respectively. Complex **6** has been prepared previously by pyrolysis of $[Co_2(CO)_6(\mu-dmpm)]$;⁵ it was stable in the solid state, but it decomposed slowly in solution at room temperature.



The solid-state structure of **6** was determined by a single-crystal X-ray analysis, which produced the atomic coordinates listed in Table III. Selected bond lengths and angles are shown in Table IV.

The molecular structure, illustrated in Figure 3, contains a distorted-tetrahedral Co_4 cluster, with two edges spanned by two dmpm ligands and one face edge-bridged by three carbonyl groups. The remaining five carbonyl ligands are essentially linear ($Co-C-O = 171.2(10)$ – $179.3(9)^\circ$). Thus, the molecular geometry of **6** can be derived from the C_{3v} structure of the parent complex $[Co_4(CO)_{12}]$,^{5,18,25} by substituting one apical and one equatorial carbonyl group with one dmpm ligand and two axial

Table III. Fractional Atomic Coordinates and Equivalent Displacement Parameters (\AA^2) for $[Co_4(CO)_5(\mu-dmpm)_2]$

	x	y	z	U^{eq}
Co(1)	0.08251(5)	-0.11372(6)	0.02914(4)	0.035
Co(2)	0.06274(6)	0.01864(7)	-0.08243(4)	0.041
Co(3)	-0.03421(5)	0.03731(7)	0.03427(4)	0.039
Co(4)	0.12935(6)	0.09623(7)	0.04393(5)	0.045
P(1)	0.00966(11)	-0.26389(14)	-0.01853(10)	0.049
P(2)	-0.01579(12)	-0.09886(18)	-0.15786(9)	0.056
P(3)	-0.06855(14)	0.16868(16)	0.12316(9)	0.055
P(4)	0.12430(14)	0.15132(21)	0.16920(11)	0.070
C(1)	0.1536(4)	-0.0922(6)	-0.0640(3)	0.049
C(2)	0.0033(5)	-0.0740(5)	0.1106(3)	0.051
C(3)	-0.0326(6)	0.1332(6)	-0.0572(3)	0.066
C(4)	0.1579(4)	-0.1925(6)	0.0860(4)	0.056
C(5)	0.1133(5)	0.0997(7)	-0.1577(4)	0.062
C(6)	-0.1421(5)	-0.0160(8)	0.0234(5)	0.077
C(7)	0.2408(5)	0.0500(8)	0.0520(5)	0.074
C(8)	0.1366(7)	0.2322(7)	-0.0043(6)	0.091
C(9)	-0.0628(5)	-0.2242(6)	-0.1027(4)	0.059
C(10)	0.0083(5)	0.1681(7)	0.2087(4)	0.064
C(11)	-0.0663(7)	-0.3357(8)	0.0522(5)	0.090
C(12)	0.0770(6)	-0.3868(7)	-0.0562(5)	0.084
C(13)	0.0483(6)	-0.1639(9)	-0.2410(4)	0.087
C(14)	-0.1147(6)	-0.0434(9)	-0.2090(5)	0.091
C(15)	-0.1756(5)	0.1438(10)	0.1769(5)	0.088
C(16)	-0.0730(10)	0.3248(8)	0.0898(6)	0.133
C(17)	0.1771(6)	0.0486(11)	0.2410(5)	0.105
C(18)	0.1808(8)	0.2900(11)	0.1913(7)	0.150
O(1)	0.2189(3)	-0.1315(5)	-0.0948(3)	0.071
O(2)	-0.0124(4)	-0.0988(5)	0.1781(3)	0.082
O(3)	-0.0670(6)	0.2116(6)	-0.0864(3)	0.118
O(4)	0.2074(4)	-0.2467(6)	0.1241(3)	0.096
O(5)	0.1462(5)	0.1495(6)	-0.2090(3)	0.107
O(6)	-0.2142(4)	-0.0506(8)	0.0166(5)	0.152
O(7)	0.3138(4)	0.0234(7)	0.0633(4)	0.111
O(8)	0.1438(7)	0.3248(6)	-0.0259(5)	0.154

$$^a U = \frac{1}{3} \sum_{i,j} h_i U_{ij} h_j^* / (h_i h_j)$$

carbonyl groups with another. The disposition of the dmpm ligands along the edges of the Co_4 tetrahedron is such as to yield the isomeric form I. The five-membered Co_2P_2C ring containing the axial dmpm ligand adopts an envelope conformation, with the CH_2 group at the flap; the conformation of the ring incorporating the C(3) and C(4) atoms is puckered, as is evident from the torsion angles shown in Table IV. The molecular structure of **6** is therefore asymmetrical and closely similar to that of the rhodium cluster $[Rh_4(CO)_8(dppm)_2]$.¹⁵

The Co–Co bond lengths in **6** vary from 2.426(1) to 2.541(2) Å and can be compared with those of 2.438(3)–2.717(1) Å observed in other crystallographically characterized cobalt complexes.^{15,18,25–29} They follow the trend displayed by tetrahedral cluster complexes of the type $[Co_4(CO)_{12-n}L_n]$ ($n = 1$ – 5), in which the metal–metal bonds in the basal plane are shorter, and presumably stronger, than the bonds involving the apical cobalt atom.^{18,26–28} In **6** the basal–basal and basal–apical Co–Co distances average 2.443 and 2.518 Å, respectively. Of the three basal–apical bonds the one spanned by the dmpm ligand (Co(3)–Co(4) = 2.541 Å) is slightly longer than the two unsupported bonds (Co(1)–Co(4) = 2.503(2) Å, Co(2)–Co(4) = 2.510 Å). In the basal plane, however, the bond bridged the dmpm ligand (Co(1)–Co(2) = 2.426(1) Å) is shorter than the other two (Co(2)–Co(3) = 2.451(2) Å, Co(1)–Co(3) = 2.452 Å).

(26) Bahoun, A. A.; Osborn, J. A.; Voelken, C.; Bonnet, J.; Lavigne, G. *Organometallics* 1982, 1, 1114.

(27) Darensbourg, D. J.; Zalewski, D. J.; Delord, T. *Organometallics* 1984, 3, 1210.

(28) Darensbourg, D. J.; Zalewski, D. J.; Rheingold, R. L.; Durney, R. L. *Inorg. Chem.* 1986, 25, 3281.

(29) Richmond, M. G.; Kochi, J. K. *Organometallics* 1987, 6, 777.

(25) (a) Wei, C. H. *Inorg. Chem.* 1969, 8, 2384. (b) Wei, C. H.; Wilkes, G. R.; Dahl, L. F. *J. Am. Chem. Soc.* 1967, 89, 4792. (c) Wei, C. H.; Dahl, L. F. *J. Am. Chem. Soc.* 1966, 88, 1821.

Table IV. Selected Interatomic Distances (Å) and Angles (deg) in $[\text{Co}_4(\text{CO})_8(\mu\text{-dmpm})_2]$

Bond Distances			
Co(1)–Co(2)	2.426(1)	Co(1)–Co(3)	2.452(2)
Co(1)–Co(4)	2.503(2)	Co(1)–P(1)	2.180(2)
Co(1)–C(1)	1.910(6)	Co(1)–C(2)	1.868(7)
Co(1)–C(4)	1.730(7)	Co(2)–Co(3)	2.451(2)
Co(2)–Co(4)	2.510(2)	Co(2)–P(2)	2.187(2)
Co(2)–C(1)	1.880(7)	Co(2)–C(3)	1.978(8)
Co(2)–C(5)	1.741(7)	Co(3)–Co(4)	2.541(2)
Co(3)–P(3)	2.177(2)	Co(3)–C(2)	1.890(7)
Co(3)–C(3)	1.888(7)	Co(3)–C(6)	1.734(8)
Co(4)–P(4)	2.202(3)	Co(4)–C(7)	1.753(8)
Co(4)–C(8)	1.751(9)	P(1)–C(9)	1.841(7)
P(2)–C(9)	1.842(8)	P(3)–C(10)	1.842(7)
P(4)–C(10)	1.867(8)		
Bond Angles			
Co(2)–Co(1)–Co(3)	60.3(1)	Co(2)–Co(1)–Co(4)	61.2(1)
Co(2)–Co(1)–P(1)	98.1(1)	Co(2)–Co(1)–C(1)	49.7(2)
Co(2)–Co(1)–C(2)	109.9(2)	Co(2)–Co(1)–C(4)	146.1(3)
Co(3)–Co(1)–Co(4)	61.7(1)	Co(3)–Co(1)–P(1)	102.0(1)
Co(3)–Co(1)–C(1)	109.6(2)	Co(3)–Co(1)–C(2)	49.7(2)
Co(3)–Co(1)–C(4)	143.9(3)	Co(4)–Co(1)–P(1)	157.7(1)
Co(4)–Co(1)–C(1)	78.7(3)	Co(4)–Co(1)–C(2)	82.7(2)
Co(4)–Co(1)–C(4)	104.9(3)	P(1)–Co(1)–C(1)	94.4(2)
P(1)–Co(1)–C(2)	98.2(3)	P(1)–Co(1)–C(4)	97.1(3)
C(1)–Co(1)–C(2)	157.6(3)	C(1)–Co(1)–C(4)	99.1(3)
C(2)–Co(1)–C(4)	97.6(3)	Co(1)–Co(2)–Co(3)	60.4(1)
Co(1)–Co(2)–Co(4)	60.9(1)	Co(1)–Co(2)–P(2)	97.8(1)
Co(1)–Co(2)–C(1)	50.7(2)	Co(1)–Co(2)–C(3)	109.3(2)
Co(1)–Co(2)–C(5)	147.1(3)	Co(3)–Co(2)–Co(4)	61.6(1)
Co(3)–Co(2)–P(2)	101.6(1)	Co(3)–Co(2)–C(1)	110.7(2)
Co(3)–Co(2)–C(3)	49.0(2)	Co(3)–Co(2)–C(5)	142.6(3)
Co(4)–Co(2)–P(2)	157.0(1)	Co(4)–Co(2)–C(1)	79.0(2)
Co(4)–Co(2)–C(3)	82.6(2)	Co(4)–Co(2)–C(5)	104.9(3)
P(2)–Co(2)–C(1)	94.2(2)	P(2)–Co(2)–C(3)	98.1(3)
P(2)–Co(2)–C(5)	97.8(3)	C(1)–Co(2)–C(3)	158.1(3)
C(1)–Co(2)–C(5)	99.3(4)	C(3)–Co(2)–C(5)	96.9(4)
C(1)–Co(3)–Co(4)	59.3(1)	Co(1)–Co(3)–Co(4)	60.2(1)
Co(1)–Co(3)–P(3)	132.4(1)	Co(1)–Co(3)–C(2)	48.9(2)
Co(1)–Co(3)–C(3)	111.6(3)	Co(1)–Co(3)–C(6)	114.4(3)
Co(2)–Co(3)–Co(4)	60.3(1)	Co(2)–Co(3)–P(3)	138.6(1)
Co(2)–Co(3)–C(2)	108.2(3)	Co(2)–Co(3)–C(3)	52.3(3)
Co(2)–Co(3)–C(6)	115.8(3)	Co(4)–Co(3)–P(3)	90.1(1)
Co(4)–Co(3)–C(6)	174.2(3)	P(3)–Co(3)–C(2)	93.6(2)
P(3)–Co(3)–C(3)	99.6(3)	P(3)–Co(3)–C(6)	95.4(3)
C(2)–Co(3)–C(3)	159.8(4)	C(2)–Co(3)–C(6)	96.5(4)
C(3)–Co(3)–C(6)	97.4(4)	Co(1)–Co(4)–Co(2)	57.9(1)
Co(1)–Co(4)–Co(3)	58.1(1)	Co(1)–Co(4)–P(4)	111.0(1)
Co(1)–Co(4)–C(7)	89.2(3)	Co(1)–Co(4)–C(8)	144.6(4)
Co(2)–Co(4)–Co(3)	58.1(1)	Co(2)–Co(4)–P(4)	154.0(1)
Co(2)–Co(4)–C(7)	109.7(3)	Co(2)–Co(4)–C(8)	86.7(4)
Co(3)–Co(4)–P(4)	95.9(1)	Co(3)–Co(4)–C(7)	147.2(3)
Co(3)–Co(4)–C(8)	105.3(4)	P(4)–Co(4)–C(7)	92.5(3)
P(4)–Co(4)–C(8)	101.2(4)	C(7)–Co(4)–C(8)	104.0(5)
Co(1)–P(1)–C(9)	112.7(3)	Co(2)–P(2)–C(9)	112.7(3)
Co(3)–P(3)–C(10)	112.8(3)	Co(4)–P(4)–C(10)	113.7(3)
Co(1)–C(1)–Co(2)	79.6(3)	Co(1)–C(2)–Co(3)	81.4(3)
Co(2)–C(3)–Co(3)	78.7(3)	P(1)–C(9)–P(2)	110.7(4)
P(3)–C(10)–P(4)	107.5(4)		
Torsion Angles			
P(1)–Co(1)–Co(2)–P(2)		0.2(1)	
Co(2)–Co(1)–P(1)–C(9)		–16.8(3)	
Co(1)–Co(2)–P(2)–C(9)		16.3(3)	
Co(1)–P(1)–C(9)–P(2)		29.8(3)	
Co(2)–P(2)–C(9)–P(1)		–29.6(3)	
P(3)–Co(3)–Co(4)–P(4)		29.9(1)	
Co(4)–Co(3)–P(3)–C(10)		–45.2(3)	
Co(3)–Co(4)–P(4)–C(10)		–13.4(3)	
Co(3)–P(3)–C(10)–P(4)		42.2(3)	
Co(4)–P(4)–C(10)–P(3)		–13.9(3)	

All the terminal Co–C distances (axial, equatorial, and apical) are equal (1.730(7)–1.753(8) Å), and they are substantially shorter than the bridging Co–C distances (1.868(7)–1.978(8) Å). Only one carbonyl bridge is slightly asymmetrical (Co(3)–C(3) = 1.888(7) Å, Co(2)–C(3) = 1.978(8) Å).

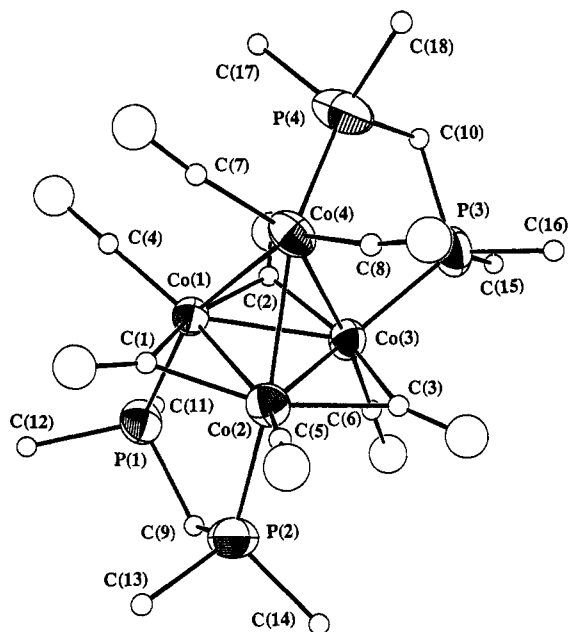


Figure 3. View of the molecular structure of $[\text{Co}_4(\text{CO})_8(\text{Me}_2\text{PCH}_2\text{PMe}_2)_2]$. The oxygen atoms are assigned the same numbers as the carbon atoms to which they are bonded, but their labels are omitted for clarity.

The Co–P bond lengths are within the range of those observed in phosphine and phosphite derivatives of the $[\text{Co}_4(\text{CO})_{12}]$ cluster (2.156(2)–2.266(6) Å).^{18,28} In the axial dmpm ligand the Co–P bonds are equal (2.180(2) and 2.187(2) Å), while for the other dmpm group the apical bond (Co(4)–P(4) = 2.202(3) Å) is substantially longer than the equatorial bond (Co(3)–P(3) = 2.177(2) Å). The lengthening of the Co(4)–P(4) bond may be attributed to the trans influence of the axial phosphine transmitted through the metal–metal bond (P(2)–Co(2)–Co(4) = 157.0(1)°, Co(2)–Co(4)–P(4) = 154.0(1)°).

The IR spectrum of 6 in the solid state gave both terminal (1989, 1963, 1946, 1930, and 1893 cm^{-1}) and bridging (1810, 1773, and 1743 cm^{-1}) carbonyl stretching frequencies, the frequencies being lower than in the parent $[\text{Co}_4(\text{CO})_{12}]$.^{16,17e} due to the strong donor ability of dmpm. In solution in CH_2Cl_2 , the carbonyl stretching frequencies were in agreement with literature data.⁵

At room temperature, the ^{31}P NMR spectrum in CD_2Cl_2 contained a broad resonance centered at δ –0.9 ppm. At –90 °C this split into three resonances with an intensity ratio of 2:1:1, consistent with the X-ray structure (Figure 4). The peaks are assigned to P^a and P^b (d, δ 6.8, $J(\text{P}^a, \text{P}^b\text{P}^d)$ = 50.4 Hz), P^c (d, δ –4.8, $J(\text{P}^c\text{P}^d)$ = 33.6 Hz), and P^d (broad, δ –11). The apical phosphorus resonance was severely broadened by the cobalt quadrupole even at low temperature.⁵ The previous report gave $\delta(\text{P})$ 11.8 at 25 °C and $\delta(\text{P})$ 12.15 (intensity 3) and 11.10 (intensity 1) at –60 °C; the chemical shifts are in poor agreement with the present data, but there is little doubt that the same complex is present. The ^1H NMR spectrum of 6 is also temperature-dependent. Thus, at room temperature, it contained a broad resonance due to the PMe protons centered at δ 1.47 but, at –90 °C, there were four such resonances as expected for the solid-state structure. These data complement the earlier report of the ^{13}C and ^{57}Co NMR spectra^{5,17} and confirm that complex 6 is fluxional.

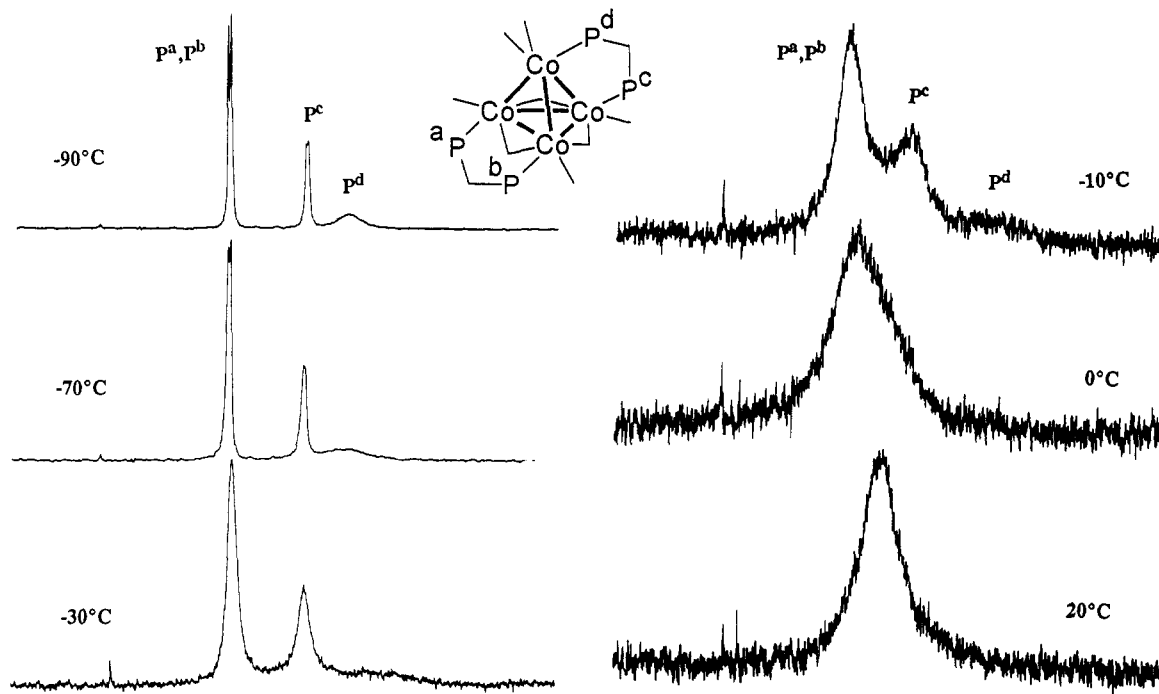
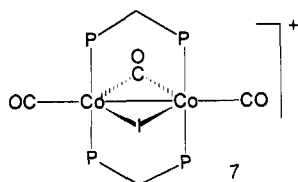


Figure 4. Variable-temperature ^{31}P NMR spectra (121 MHz) for $[\text{Co}_4(\text{CO})_8(\text{Me}_2\text{PCH}_2\text{PMe}_2)_2]$. The chemical shifts at -90°C are δ 6.8 [P^a, P^b], -4.8 [P^c], -11 [P^d].

Reaction Chemistry of $[\text{Co}_2(\text{CO})_4(\mu\text{-dmpm})_2]$

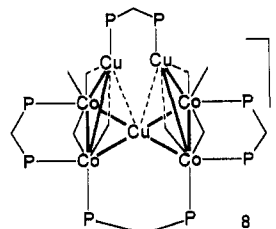
A study of the reaction of 1a/2a was made with the expectation that the small, strong donor ligands dmpm would lead to easy oxidation of cobalt.^{5,7,27-35}

$[\text{Co}_2(\text{CO})_4(\mu\text{-dmpm})_2]$ reacted easily with iodine, and following precipitation with NaBPh_4 , the red crystalline complex $[\text{Co}_2(\mu\text{-I})(\text{CO})_2(\mu\text{-CO})(\mu\text{-dmpm})_2][\text{BPh}_4]$ (7) was isolated. Complex 7 was also formed on reaction of 1a/2a with sodium iodide and NaBPh_4 ; clearly it is easily oxidized. A number of complexes similar to 7 are known,²² and it was readily characterized by its analytical and spectroscopic data (see Experimental Section).



Reaction of 1a/2a with $[\text{Cu}(\text{MeCN})_4]\text{BF}_4$ gave a deep green solution from which black, air-stable crystals of $[\text{Co}_4\text{Cu}_3(\text{CO})_8(\mu\text{-dmpm})_4]\text{BF}_4$ (8) were isolated in low yield. Since the spectroscopic data did not define the structure, it was characterized by an X-ray structure determination.

The molecular structure of the cluster cation 8 is illustrated in Figure 5. Positional parameters and bond distances and angles are given in Tables V and VI. The cluster core can be considered to comprise two triangles



of metal atoms ($\text{Co}(1)\text{Co}(2)\text{Cu}(2)$ and $\text{Co}(3)\text{Co}(4)\text{Cu}(3)$) bridged by a central copper atom ($\text{Cu}(1)$). Each Co_2Cu triangle has three edge-bridging carbonyl ligands, of which one (e.g. $\text{C}(3)\text{O}(3)$) bridges a $\text{Co}\text{-Co}$ bond and two (e.g. $\text{C}(5)\text{O}(5)$ and $\text{C}(7)\text{O}(7)$) are semibridging between cobalt and copper.^{36,37} The two Co_2Cu triangles are bridged by two dmpm ligands, of which one bridges between equivalent copper atoms ($\text{Cu}(2)\text{P}(1)\text{P}(2)\text{Cu}(3)$) and one bridges between cobalt atoms ($\text{Co}(1)\text{P}(3)\text{P}(4)\text{Co}(3)$). The other two dmpm ligands bridge between cobalt atoms within each Co_2Cu triangle (e.g. $\text{Co}(1)\text{P}(5)\text{P}(6)\text{Co}(2)$). There are two terminal carbonyls bound to cobalt ($\text{Co}(2)\text{C}(1)\text{O}(1)$, $\text{Co}(4)\text{C}(2)\text{O}(2)$). The two Co_2Cu triangles lean toward one another such that the nonbonded distance $\text{Cu}(2)\text{-Cu}(3) = 3.211(4)$ Å is much shorter than the corresponding distances $\text{Co}(1)\text{-Co}(3) = 4.248(4)$ Å and $\text{Co}(2)\text{-Co}(4) = 4.24(4)$ Å. In order to span the long $\text{Co}(1)\text{-Co}(3)$ distance, the $\mu\text{-dmpm}$ ligand has bond angles which are significantly distorted from the normal tetrahedral values (e.g. $\text{P}(3)\text{-C}(20)\text{-P}(4) = 121.8(2.1)^\circ$; $\text{Co}(3)\text{-P}(4)\text{-C}(20) = 121.5(1.4)^\circ$). Indeed, the cluster is remarkable in having the versatile $\mu\text{-dmpm}$ ligands spanning pairs of metal atoms separated by the disparate distances of 2.51, 2.52, 3.21, and 4.25 Å.

The most remarkable feature of the structure of 8 is the geometry of the bridging copper atom $\text{Cu}(1)$. It does not bridge symmetrically between the faces of the Co_2Cu

(30) Hanson, B. E.; Fanwick, P. E.; Mancini, J. S. *Inorg. Chem.* 1982, 21, 3811.

(31) Puddephatt, R. J.; Thompson, M. A.; Manojlović-Muir, L.; Muir, K. W.; Frew, A. A.; Brown, M. P. *J. Chem. Soc., Chem. Commun.* 1981, 805.

(32) Ling, S. S. M.; Puddephatt, R. J.; Manojlović-Muir, L.; Muir, K. W. *Inorg. Chim. Acta* 1983, 77, L95.

(33) Ling, S. S. M.; Jobe, I. R.; McLennan, A. J.; Manojlović-Muir, L.; Muir, K. W.; Puddephatt, R. J. *J. Chem. Soc., Chem. Commun.* 1985, 566.

(34) King, R. B.; Raghuvveer, K. S. *Inorg. Chem.* 1984, 23, 2482.

(35) Puddephatt, R. J. *Chem. Soc. Rev.* 1983, 99.

(36) Darensbourg, D. J.; Chao, C.-S.; Reibenspies, J. H.; Bischoff, C. *J. Inorg. Chem.* 1990, 29, 2153.

(37) Achternbosch, M.; Braun, H.; Fuchs, R.; Klufers, P.; Selle, A.; Wilhelm, V. *Angew. Chem., Int. Ed. Engl.* 1990, 29, 783.

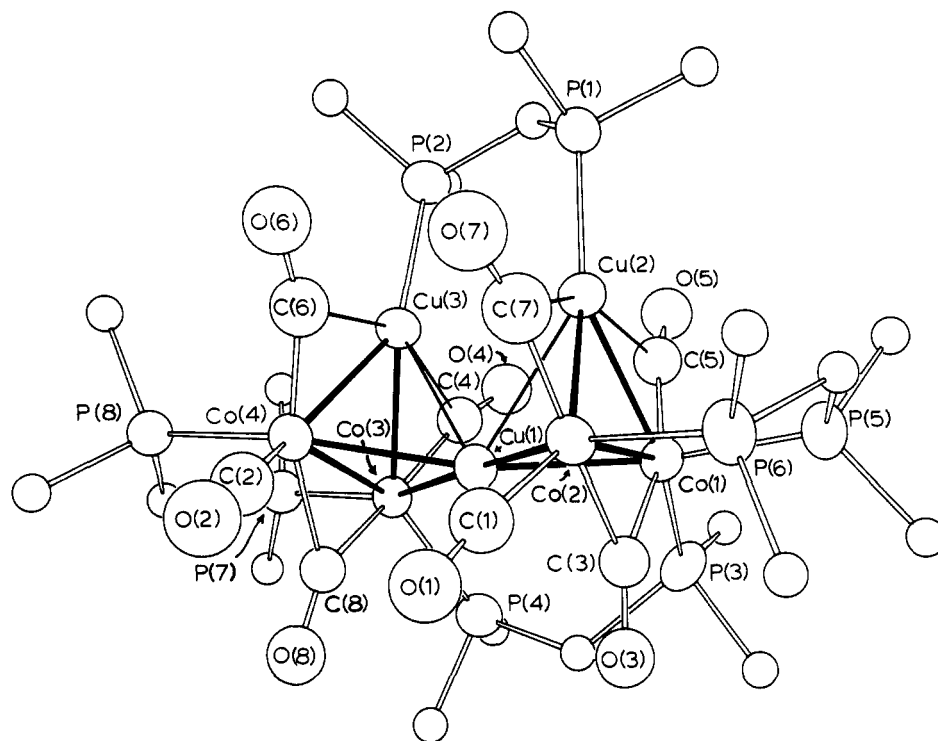


Figure 5. View of the structure of the cluster cation $[\text{Co}_4\text{Cu}_3(\text{CO})_8(\mu\text{-dmpm})_4]^+$.

triangles but is displaced toward the cobalt atoms such that the Cu(1)–Co distances (2.458(4)–2.474(4) Å) are significantly shorter than the Cu(1)–Cu distances (2.683(4) and 2.624(3) Å). The latter distances are in the range found for weak lateral forces between copper(I) atoms,^{38,39} but the Cu–Cu bonding is still presumably partly responsible for the tilting of the Co_2Cu triangles described above. The four cobalt atoms and Cu(1) are approximately coplanar (dihedral angle between planes Cu(1)Co(1)Co(2) and Cu(1)Co(3)Co(4) 14.8(3)°; Co(2)–Cu(1)–Co(3) = 178.0(1)°, Co(1)–Cu(1)–Co(4) = 168.1(1)°). Although at least one group 11 cluster complex is known to contain an approximately square-planar metal center in oxidation state I,⁴⁰ this stereochemistry is much more typical of these metals in oxidation state III. Furthermore, formal removal of the central copper atom Cu(1) as Cu^+ leaves each Co_2Cu triangle with an odd electron count, whereas its removal as Cu^{3+} and the other copper atoms as LCu^+ leaves two $[\text{Co}_2\text{L}_6(\mu\text{-CO})]^{2-}$ units (where L = terminal CO or phosphine donor atoms) in which cobalt has an 18-electron configuration and each Co_2Cu triangle has its favored electron count.³⁹ Although the use of oxidation states in clusters is fraught with problems, it is used here to indicate that the atom Cu(1) probably uses dsp^2 hybrid orbitals in bonding and has the stereochemistry expected for this bonding state. Together these factors suggest that the cluster contains a formally d^8 copper(III) atom (Cu(1)). The presence of square-planar copper in cluster complexes appears to be unprecedented.³⁹

Since the electron configuration of the cluster was unexpected, the possible presence of hydride ligands was considered. It should be noted that a formulation as $[\text{Co}_4\text{Cu}_3\text{H}_2(\text{CO})_8(\mu\text{-dmpm})_4]^+$ would require Cu(1) to have oxidation state I. However, no evidence for hydride was

observed in the ^1H NMR spectrum (no signals from δ 0 to $-\infty$) or from final difference Fourier maps in the X-ray structure determination. Dissolution of the cluster in a $[\text{D}_7\text{H}_7]$ dimethylformamide/ CCl_4 mixture failed to give any trace of CHCl_3 . This reduction of CCl_4 to CHCl_3 is a sensitive test for transition-metal hydrides. The mass spectrum gave a peak at m/z 1195 as expected for the cluster cation without hydride ligands. Hence, hydride ligands are presumed to be absent.

Cluster 8 dissolved only in highly polar solvents such as *N,N*-dimethylformamide, and the solutions were very air-sensitive. The ^{31}P NMR spectrum of 8 in DMF solution contained three resonances with an intensity ratio of 1:2:1 at δ 3.66, 3.28, and -31.19 , respectively, fully consistent with the solid-state structure. The resonance at δ 3.66 is assigned to the dmpm ligand bridging cobalt atoms between the two Co_2Cu triangles and the resonance at δ 3.28 is attributed to the dmpm ligands bridging the Co–Co bonds within each Co_2Cu triangle, while the resonance at δ -31.19 is attributed to the dmpm ligand bridging the two copper atoms. The ^1H NMR spectrum contained six resonances for PMe protons with an intensity ratio of 1:1:1:1:1:2 at δ 1.04, 1.18, 1.24, 1.42, 1.64, and 1.68 ppm, respectively, again consistent with the solid-state structure.

The IR spectrum of 8 contained carbonyl stretching bands in three distinct regions. Bands at 1981, 1946, and 1917 cm^{-1} are assigned to terminally bound CO and bands at 1879, 1860, 1838, 1833, and 1803 cm^{-1} are assigned to semibridging CO, while a band at 1713 cm^{-1} is assigned to bridging CO.^{5,27,30} Similar stretching frequencies for semibridging carbonyls were earlier reported in other mixed-metal cobalt complexes such as $[(\text{tmed})\text{CuCo}(\text{CO})_4]$ (tmed = *N,N,N',N'*-tetramethylethylenediamine),⁴¹ $[\text{Cu}(\text{dmpe})_2][\text{Cu}(\text{Co}(\text{CO})_4)_2]$,³⁶ and $[\text{CoRh}(\text{CO})_8(\text{dppm})_2]$.⁴²

The FAB mass spectrum of 8 gave a parent ion peak for $\text{Co}_4\text{Cu}_3(\text{CO})_8(\text{dmpm})_4^+$ at m/e 1195, with an excellent

(38) Lee, S. W.; Troglor, W. C. *Inorg. Chem.* 1990, 29, 1659.

(39) Salter, I. *Adv. Organomet. Chem.* 1989, 249.

(40) Johnson, B. F. G.; Kaner, D. A.; Lewis, J.; Raithby, P. R. *J. Chem. Soc., Chem. Commun.* 1981, 753.

(41) Doyle, G.; Eriksen, K. A.; VanEngen, D. *Organometallics* 1985, 4, 877.

Table V. Atomic Positional and Thermal Parameters (\AA^2) for $[\text{Co}_4\text{Cu}_3(\text{CO})_8(\mu\text{-dmpm})_4]\text{BF}_4$

atom	x	y	z	U or U_{eq}^a
Cu(1)	0.3786(2)	0.4965(1)	0.2648(1)	0.0346(8)*
Cu(2)	0.4129(2)	0.6288(1)	0.2667(1)	0.0375(8)*
Cu(3)	0.2342(2)	0.5415(1)	0.3477(1)	0.0375(8)*
Co(1)	0.3689(2)	0.5664(1)	0.1741(1)	0.0326(8)*
Co(2)	0.5704(2)	0.5520(1)	0.2343(1)	0.0353(9)*
Co(3)	0.1908(2)	0.4373(1)	0.2947(1)	0.0312(8)*
Co(4)	0.3749(2)	0.4478(1)	0.3664(1)	0.0351(9)*
P(1)	0.3595(6)	0.7177(3)	0.3192(2)	0.045(2)*
P(2)	0.1577(6)	0.6366(3)	0.3824(3)	0.052(2)*
P(3)	0.2363(5)	0.5087(3)	0.1179(2)	0.044(2)*
P(4)	0.1444(5)	0.3949(3)	0.2054(3)	0.042(2)*
P(5)	0.4379(5)	0.6396(3)	0.1089(3)	0.044(2)*
P(6)	0.6854(5)	0.6083(3)	0.1729(3)	0.044(2)*
P(7)	0.0654(5)	0.3866(3)	0.3573(2)	0.042(2)*
P(8)	0.2955(5)	0.3930(3)	0.4413(2)	0.039(2)*
C(10)	0.197(2)	0.713(1)	0.346(1)	0.079(8)
C(11)	0.450(2)	0.741(1)	0.382(1)	0.12(1)
C(12)	0.347(2)	0.795(1)	0.279(1)	0.093(9)
C(21)	-0.008(2)	0.644(1)	0.375(1)	0.12(1)
C(22)	0.185(2)	0.650(1)	0.460(1)	0.10(1)
C(20)	0.225(4)	0.417(2)	0.144(2)	0.16(2)
C(31)	0.283(3)	0.479(1)	0.048(1)	0.08(1)
C(32)	0.101(3)	0.543(2)	0.098(1)	0.19(2)
C(41)	-0.007(3)	0.378(2)	0.185(1)	0.18(2)
C(42)	0.178(4)	0.312(2)	0.196(2)	0.19(2)
C(30)	0.592(2)	0.672(1)	0.1340(9)	0.058(7)
C(51)	0.466(2)	0.618(1)	0.0296(9)	0.095(9)
C(52)	0.354(2)	0.716(1)	0.098(1)	0.10(1)
C(61)	0.812(2)	0.658(1)	0.202(1)	0.081(8)
C(62)	0.756(2)	0.560(1)	0.1160(9)	0.091(9)
C(40)	0.155(2)	0.345(1)	0.4170(9)	0.056(6)
C(71)	-0.046(2)	0.320(1)	0.3386(9)	0.069(7)
C(72)	-0.036(2)	0.444(1)	0.3960(9)	0.064(7)
C(81)	0.386(2)	0.327(1)	0.4771(8)	0.059(7)
C(82)	0.246(2)	0.442(1)	0.5057(9)	0.077(8)
O(1)	0.745(1)	0.4458(8)	0.2641(6)	0.070(5)
O(1)	0.673(2)	0.489(1)	0.2552(9)	0.059(7)
O(2)	0.626(2)	0.3985(8)	0.3787(7)	0.086(6)
O(2)	0.528(2)	0.419(1)	0.373(1)	0.064(7)
O(3)	0.520(1)	0.4545(7)	0.1415(6)	0.056(4)
O(3)	0.492(2)	0.503(1)	0.1686(8)	0.043(6)
O(4)	0.008(1)	0.5394(7)	0.2659(6)	0.060(4)
O(4)	0.092(2)	0.504(1)	0.2828(8)	0.047(6)
O(5)	0.163(1)	0.6503(7)	0.2084(6)	0.055(4)
O(5)	0.257(2)	0.619(1)	0.2017(9)	0.045(6)
O(6)	0.443(1)	0.5645(8)	0.4365(7)	0.078(5)
O(6)	0.397(2)	0.524(1)	0.401(1)	0.062(7)
O(7)	0.649(2)	0.6237(8)	0.3406(7)	0.089(6)
O(7)	0.598(2)	0.601(1)	0.297(1)	0.073(8)
O(8)	0.366(1)	0.3268(7)	0.2953(6)	0.063(5)
O(8)	0.327(2)	0.381(1)	0.3086(8)	0.039(6)
B	0.051(1)	0.1927(9)	0.5030(7)	0.14(4)
F(1)	-0.051(1)	0.2230(9)	0.4759(7)	0.195(8)
F(2)	0.015(1)	0.1346(9)	0.5293(7)	0.195(8)
F(3)	0.103(1)	0.2342(9)	0.5458(7)	0.195(8)
F(4)	0.137(1)	0.1790(9)	0.4610(7)	0.195(8)
B'	0.034(3)	0.185(1)	0.514(1)	0.2(2)
F(1')	-0.061(3)	0.190(1)	0.547(1)	0.040(8)
F(2')	0.095(3)	0.133(1)	0.507(1)	0.040(8)
F(3')	-0.010(3)	0.210(1)	0.453(1)	0.040(8)
F(4')	0.118(3)	0.241(1)	0.529(1)	0.040(8)
B''	0.067(4)	0.181(2)	0.499(2)	0.01(1)
F(1'')	0.031(4)	0.199(2)	0.442(2)	0.01(1)
F(2'')	0.040(4)	0.116(2)	0.508(2)	0.01(1)
F(3'')	0.004(4)	0.220(2)	0.539(2)	0.01(1)
F(4'')	0.192(4)	0.191(2)	0.507(2)	0.01(1)

^a Parameters with an asterisk were refined anisotropically and are given in the form of the isotropic equivalent displacement parameter defined as $U_{\text{eq}} = \frac{1}{3} \sum_i \sum_j U_{ij} a_i^* a_j^* (\mathbf{a}_i \cdot \mathbf{a}_j)$.

agreement between observed and calculated isotope patterns. In addition, EDX analysis confirmed the cobalt to

copper ratio of 4:3. Thus, all of this evidence is fully consistent with the solid-state structure for 8.

Complex 8 was obtained in only low yield along with numerous unidentified compounds, and attempts to prepare analogous silver and gold derivatives were unsuccessful. The stoichiometry and mechanism of formation of 8 therefore remain obscure.

Experimental Section

NMR spectra were recorded in CD_2Cl_2 unless otherwise specified, using varian XL200 or XL300 spectrometers. Chemical shifts are quoted with respect to TMS or external H_3PO_4 .

$[\text{Co}_2(\text{CO})_2(\mu\text{-CO})_2(\mu\text{-dmpm})_2]$ (1a). $\text{CoCl}_2 \cdot 6\text{H}_2\text{O}$ (0.5 g, 2.1 mmol) was dissolved in EtOH (60 mL), and dmpm (0.8 mL, 6.95 mmol) was added. The resulting yellow-brown mixture was stirred under a slow stream of CO gas for 1 h. An ethanolic suspension (20 mL) of NaBH_4 (0.35 g, 9.25 mmol) was added dropwise over a period of 15 min. The mixture was stirred for a further 2.5 h under a slow stream of CO gas to give a yellow-orange suspension. This was filtered off and recrystallized from CH_2Cl_2 (10 mL)/*n*-pentane (20 mL) to give the yellow-orange microcrystalline product, which was washed with EtOH (7 mL) and dried under vacuum: yield 20%; mp 135–137 °C. Anal. Calcd for $\text{C}_{14}\text{H}_{28}\text{O}_4\text{P}_4\text{Co}_2$: C, 33.53; H, 5.59. Found: C, 32.85; H, 5.71. IR (CH_2Cl_2): 1a, 1945, 1916, 1735 cm^{-1} ; 2a, 1953, 1920, 1893 cm^{-1} . NMR at -92 °C in CD_2Cl_2 for 1a: δ (¹H) 1.93 [m, 2H, $\text{CH}^*\text{H}^b\text{P}_2$], 2.75 [m, 2H, $\text{CH}^*\text{H}^b\text{P}_2$], 1.50 [overlapping m, 24H, MeP]; δ (¹³C) 203.5 [terminal CO], 265.5 [$\mu\text{-CO}$], 19.5, 19.0 [MeP]; δ (³¹P) 29.85 [s, dmpm]. NMR at -62 °C CD_2Cl_2 for 2a: δ (³¹P) 19.3 [br s, dmpm]. FAB-MS: *m/z* 502, calcd for $\text{Co}_2(\text{CO})_4(\text{dmpm})_2^+$ 502.

$[\text{Co}_4(\text{CO})_8(\mu\text{-dmpm})_2]$ (6). To a solution of $\text{CoCl}_2 \cdot 6\text{H}_2\text{O}$ (0.90 g, 2.75 mmol) in EtOH (60 mL) was added dmpm (0.40 mL, 3.47 mmol). This solution was then saturated with CO gas for 0.5 h, and a suspension of NaBH_4 (0.40 g, 10.57 mmol) in EtOH (20 mL) was added over a period of 15 min. The black reaction mixture was stirred under CO for 2.5 h, and the solvent was evaporated under vacuum to give the black product, which was recrystallized from benzene/*n*-heptane: yield 15%. Anal. Calcd for $\text{C}_{18}\text{H}_{28}\text{O}_8\text{P}_4\text{Co}_4 \cdot 0.5\text{C}_7\text{H}_{16}$: C, 33.0; H, 4.6. Found: C, 33.7; H, 3.3 (heptane confirmed by NMR). IR (Nujol): $\nu(\text{CO})$ 1989, 1963, 1946, 1930, 1893 cm^{-1} [terminal CO]; 1810, 1773, 1743 cm^{-1} [$\mu\text{-CO}$]. NMR in CD_2Cl_2 : δ (¹H) (25 °C) 2.45 [br, CH_2P_2], 1.47 [d, $J(\text{PH})_{\text{obs}} = 8$ Hz, PMe_2]; δ (¹H) (-90 °C) 3.17 [br t, $\text{CH}^*\text{H}^b\text{P}_2$, $J(\text{PH}) = 9.5$ Hz], 2.05 [br, $\text{CH}^*\text{H}^b\text{P}_2$, H^b], the resonance due to H^a is hidden, 1.64 [br d, PMe_2 , $J(\text{PH})_{\text{obs}} = 7$ Hz], 1.49 [br, PMe_2], 1.34 [br, PMe_2], 1.23 [br d, PMe_2 , $J(\text{PH})_{\text{obs}} = 7.5$ Hz]; δ (³¹P) (25 °C) -0.9 [br s, dmpm]; δ (³¹P) (-90 °C) 6.8 [d, $J(\text{PP}) = 50.4$ Hz, P^aP^b], -4.8 [br d, $J(\text{PP}) = 33.6$ Hz, P^c], -11 [br, P^d].

$[\text{Co}_2(\mu\text{-I})(\text{CO})_2(\mu\text{-CO})(\mu\text{-dmpm})_2]\text{BPh}_4$ (7). To a solution of $[\text{Co}_2(\text{CO})_4(\mu\text{-dmpm})_2]$ (0.16 g, 0.32 mmol) in $\text{C}_2\text{H}_4\text{Cl}_2$ (7 mL) was added a solution of NaI (0.1 g, 0.67 mmol) in ethanol (3 mL). The mixture was stirred overnight, forming a red solution with some white precipitate. The solution was filtered, excess NaBPh_4 in ethanol was added to the filtrate, and a layer of ethanol (15 mL) was added. The red crystalline product which precipitated was filtered off, washed with *n*-pentane (10 mL), and dried under vacuum: yield 20%; mp 133–135 °C dec. Anal. Calcd for $\text{C}_{37}\text{H}_{48}\text{BIO}_3\text{P}_4\text{Co}_2 \cdot 1.25\text{CH}_2\text{Cl}_2$: C, 44.73; H, 4.92. Found: C, 44.74; H, 5.37. IR (Nujol): $\nu(\text{CO})$ 2018 (vw), 1937 (vs), 1901 (sh), 1804 (vs) cm^{-1} . NMR at 25 °C in CD_2Cl_2 : δ (¹H) 1.7 [d, PMe], 2.4 m, $\text{CH}^*\text{H}^b\text{P}_2$, $J(\text{PH}) = 5.5$ Hz], 2.68 [m, $\text{CH}^*\text{H}^b\text{P}_2$, $J(\text{PH}) = 5.5$ Hz], 7.4 [m, BPh]; δ (³¹P) 29.3 [s, dmpm].

$[\text{Co}_4\text{Cu}_3(\text{CO})_8(\mu\text{-dmpm})_4]\text{BF}_4$ (8). To a solution of $[\text{Co}_2(\text{CO})_4(\text{dmpm})_2]$ (0.70 g, 0.14 mmol) in CH_2Cl_2 (10 mL) was added a suspension of $[\text{Cu}(\text{MeCN})_4]\text{BF}_4$ (0.05 g, 0.14 mmol) in CH_2Cl_2 (5 mL). The original dark brown solution immediately turned deep green. The mixture was stirred for a further 4 h under a N_2 atmosphere. The green solution was decanted from insoluble material, and a layer of *n*-pentane was added. The

Table VI. Selected Bond Distances (Å) and Angles (deg) for $[\text{Co}_4\text{Cu}_3(\text{CO})_8(\mu\text{-dmpm})_4]\text{BF}_4$

Bond Distances							
Cu(2)–Cu(1)	2.683(4)	Cu(3)–Cu(1)	2.624(3)	C(6)–Cu(3)	2.12(2)	P(3)–Co(1)	2.196(6)
Co(1)–Cu(1)	2.466(4)	Co(2)–Cu(1)	2.463(4)	P(5)–Co(1)	2.219(6)	C(3)–Co(1)	1.84(2)
Co(3)–Cu(1)	2.458(4)	Co(4)–Cu(1)	2.474(4)	C(5)–Co(1)	1.73(2)	P(6)–Co(2)	2.196(6)
Cu(3)–Cu(2)	3.221(4)	Co(1)–Cu(2)	2.450(4)	C(1)–Co(2)	1.73(2)	C(3)–Co(2)	1.93(2)
Co(2)–Cu(2)	2.422(4)	Co(3)–Cu(2)	2.443(3)	C(7)–Co(2)	1.73(3)	P(4)–Co(3)	2.209(6)
Co(4)–Cu(2)	2.442(4)	Co(2)–Co(1)	2.523(4)	P(7)–Co(3)	2.228(6)	C(4)–Co(3)	1.73(2)
Co(4)–Co(3)	2.509(4)	P(1)–Cu(2)	2.223(6)	C(8)–Co(3)	1.87(2)	P(8)–Co(4)	2.202(6)
P(2)–Cu(3)	2.229(6)	C(5)–Cu(2)	2.19(2)	C(2)–Co(4)	1.75(2)	C(6)–Co(4)	1.73(2)
C(7)–Cu(2)	2.15(2)	C(4)–Cu(3)	2.20(2)	C(8)–Co(4)	1.92(2)		
Bond Angles							
Cu(3)–Cu(1)–Cu(2)	74.5(1)	Co(1)–Cu(1)–Cu(2)	56.6(1)	C(3)–Co(2)–Co(1)	46.4(6)	C(3)–Co(2)–P(6)	91.6(6)
Co(1)–Cu(1)–Cu(3)	112.1(1)	Co(2)–Cu(1)–Cu(2)	55.96(9)	C(3)–Co(2)–C(1)	95.2(9)	C(7)–Co(2)–Cu(1)	98.7(8)
Co(2)–Cu(1)–Cu(3)	124.3(1)	Co(2)–Cu(1)–Co(1)	61.6(1)	C(7)–Co(2)–Cu(2)	59.5(8)	C(7)–Co(2)–Co(1)	118.7(8)
Co(3)–Cu(1)–Cu(2)	126.1(1)	Co(3)–Cu(1)–Co(3)	57.35(9)	C(7)–Co(2)–P(6)	97.5(8)	C(7)–Co(2)–C(1)	96(1)
Co(3)–Cu(1)–Co(1)	119.3(1)	Co(3)–Cu(1)–Co(2)	178.0(1)	C(7)–Co(2)–C(3)	164(1)	Cu(3)–Co(3)–Cu(1)	64.7(1)
Co(4)–Cu(1)–Cu(2)	112.6(1)	Co(4)–Cu(1)–Cu(3)	57.2(1)	Co(4)–Co(3)–Cu(1)	59.8(1)	Co(4)–Co(3)–Cu(3)	59.1(1)
Co(4)–Cu(1)–Co(1)	168.1(1)	Co(4)–Cu(1)–Co(2)	118.4(1)	P(4)–Co(3)–Cu(1)	95.8(2)	P(4)–Co(3)–Cu(3)	143.3(2)
Co(4)–Cu(1)–Co(3)	61.2(1)	Co(1)–Cu(2)–Cu(1)	57.2(1)	P(4)–Co(3)–Co(4)	139.0(2)	P(7)–Co(3)–Cu(1)	156.2(2)
Co(2)–Cu(2)–Cu(1)	57.4(1)	Co(2)–Cu(2)–Co(1)	62.4(1)	P(7)–Co(3)–Cu(3)	101.3(2)	P(7)–Co(3)–Co(4)	96.8(2)
P(1)–Cu(2)–Cu(1)	140.0(2)	P(1)–Cu(2)–Co(1)	144.2(2)	P(7)–Co(3)–P(4)	105.7(2)	C(4)–Co(3)–Cu(1)	95.2(7)
P(1)–Cu(2)–Co(2)	150.1(2)	C(5)–Cu(2)–Cu(1)	78.4(5)	C(4)–Co(3)–Cu(3)	61.0(7)	C(4)–Co(3)–Co(4)	120.0(7)
C(5)–Cu(2)–Co(1)	43.5(5)	C(5)–Cu(2)–Co(2)	105.8(6)	C(4)–Co(3)–P(7)	92.5(7)	C(4)–Co(3)–P(7)	93.9(7)
C(5)–Cu(2)–P(1)	102.5(6)	C(7)–Cu(2)–Cu(1)	82.8(7)	C(8)–Co(3)–Cu(1)	72.2(6)	C(8)–Co(3)–Cu(3)	107.9(6)
C(7)–Cu(2)–Co(1)	106.4(7)	C(7)–Cu(2)–Co(2)	44.1(7)	C(8)–Co(3)–Co(4)	49.5(6)	C(8)–Co(3)–P(4)	93.7(6)
C(7)–Cu(2)–P(1)	107.1(7)	C(7)–Cu(2)–C(5)	149.9(9)	C(8)–Co(3)–P(7)	96.0(6)	C(8)–Co(3)–C(4)	166.5(9)
Co(3)–Cu(3)–Cu(1)	57.90(9)	Co(4)–Cu(3)–Cu(1)	58.3(1)	Cu(3)–Co(4)–Cu(1)	64.5(1)	Co(3)–Co(4)–Cu(1)	59.1(1)
Co(4)–Cu(3)–Co(3)	61.8(1)	P(2)–Cu(3)–Cu(1)	141.0(2)	Co(3)–Co(4)–Cu(3)	59.1(1)	P(8)–Co(4)–Cu(1)	156.3(2)
P(2)–Cu(3)–Co(3)	146.8(2)	P(2)–Cu(3)–Co(4)	146.7(2)	P(8)–Co(4)–Cu(3)	105.0(2)	P(8)–Co(4)–Co(3)	97.2(2)
C(4)–Cu(3)–Cu(1)	80.4(5)	C(4)–Cu(3)–Co(3)	43.3(6)	C(2)–Co(4)–Cu(1)	99.1(7)	C(2)–Co(4)–Cu(3)	147.8(8)
C(4)–Cu(3)–Co(4)	105.1(6)	C(4)–Cu(3)–P(2)	105.3(6)	C(2)–Co(4)–Co(3)	138.0(8)	C(2)–Co(4)–P(8)	99.4(7)
C(6)–Cu(3)–Cu(1)	81.0(6)	C(6)–Cu(3)–Co(3)	105.8(6)	C(6)–Co(4)–Cu(1)	93.3(7)	C(6)–Co(4)–Cu(3)	58.0(7)
C(6)–Cu(3)–Co(4)	44.0(6)	C(6)–Cu(3)–P(2)	104.7(7)	C(6)–Co(4)–Co(3)	117.1(8)	C(6)–Co(4)–P(8)	98.6(7)
C(6)–Cu(3)–C(4)	149.1(9)	Cu(2)–Co(1)–Cu(1)	66.2(1)	C(6)–Co(4)–C(2)	98.2(1)	C(8)–Co(4)–Cu(1)	71.0(6)
Co(2)–Co(1)–Cu(1)	59.2(1)	Co(2)–Co(1)–Cu(2)	58.3(1)	C(8)–Co(4)–Cu(3)	106.0(6)	C(8)–Co(4)–Co(3)	47.6(6)
P(3)–Co(1)–Cu(1)	100.2(2)	P(3)–Co(1)–Cu(2)	148.7(2)	C(8)–Co(4)–P(8)	93.4(6)	C(8)–Co(4)–C(2)	93.1(1)
P(3)–Co(1)–Co(2)	140.4(2)	P(5)–Co(1)–Cu(1)	156.0(2)	C(8)–Co(4)–C(6)	162.0(9)	P(2)–C(10)–P(1)	115(1)
P(5)–Co(1)–Cu(2)	99.1(2)	P(5)–Co(1)–Co(2)	97.2(2)	P(4)–C(20)–P(3)	122(2)	P(6)–C(30)–P(5)	111(1)
P(5)–Co(1)–P(3)	101.5(2)	C(3)–Co(1)–Cu(1)	69.7(6)	P(8)–C(40)–P(7)	112(1)	O(1)–C(1)–Co(2)	174(2)
C(3)–Co(1)–Cu(2)	107.1(6)	C(3)–Co(1)–Co(2)	49.7(6)	O(2)–C(2)–Co(4)	177(2)	Co(2)–C(3)–Co(1)	83.9(8)
C(3)–Co(1)–P(3)	92.8(6)	C(3)–Co(1)–P(5)	98.9(6)	O(3)–C(3)–Co(1)	143(2)	O(3)–C(3)–Co(2)	133(2)
C(5)–Co(1)–Cu(1)	93.6(7)	C(5)–Co(1)–Cu(2)	60.2(7)	Co(3)–C(4)–Cu(3)	75.7(8)	O(4)–C(4)–Cu(3)	120(2)
C(5)–Co(1)–Co(2)	118.4(7)	C(5)–Co(1)–P(3)	94.6(7)	O(4)–C(4)–Co(3)	164(2)	Co(1)–C(5)–Cu(2)	76.4(8)
C(5)–Co(1)–P(5)	94.9(7)	C(5)–Co(1)–C(3)	162.8(9)	O(5)–C(5)–Cu(2)	120(2)	O(5)–C(5)–Co(1)	164(2)
Cu(2)–Co(2)–Cu(1)	66.6(1)	Co(1)–Co(2)–Cu(1)	59.3(1)	Co(4)–C(6)–Cu(3)	78.1(9)	O(6)–C(6)–Cu(3)	124(2)
Co(1)–Co(2)–Cu(2)	59.4(1)	P(6)–Co(2)–Cu(1)	154.6(2)	O(6)–C(6)–P(4)	157.7(2)	Co(2)–C(7)–Cu(2)	76.4(1)
P(6)–Co(2)–Cu(2)	106.0(2)	P(6)–Co(2)–Co(1)	95.7(2)	O(7)–C(7)–Cu(2)	124(2)	O(7)–C(7)–Co(2)	160(2)
C(1)–Co(2)–Cu(1)	97.2(7)	C(1)–Co(2)–Cu(2)	146.2(7)	Co(4)–C(8)–Co(3)	82.9(8)	O(8)–C(8)–Co(3)	142(2)
C(1)–Co(2)–Co(1)	138.8(7)	C(1)–Co(2)–P(6)	100.2(7)	O(8)–C(8)–Co(4)	135(2)		
C(3)–Co(2)–Cu(1)	68.5(6)	C(3)–Co(2)–Cu(2)	105.0(6)				
Torsion Angles							
Co(3)–Cu(1)–Co(1)–Co(2)	–177.9(2)			Co(4)–Cu(1)–Co(1)–Co(2)	93.4(7)		
Co(3)–Cu(1)–Co(2)–Co(1)	116(4)			Co(4)–Cu(1)–Co(2)–Co(1)	–166.4(2)		
Co(1)–Cu(1)–Co(3)–Co(4)	–166.4(2)			Co(2)–Cu(1)–Co(3)–Co(4)	79(4)		
Co(1)–Cu(1)–Co(4)–Co(3)	95.4(7)			Co(2)–Cu(1)–Co(4)–Co(3)	–177.7(2)		

intensely green crystalline product (large crystals appear black) separated; it was washed with *n*-pentane and dried under reduced pressure: yield 5%; mp 174–175 °C dec. IR (Nujol): $\nu(\text{CO})$ 1981 (vs), 1946 (m), 1917 (sh), 1879 (vs), 1860 (vs), 1838 (m), 1833 (m), 1803 (sh), 1713 (vs) cm^{-1} . NMR at 25 °C in DMF-*d*₇: $\delta(\text{H})$ 1.04 [3H, Me], 1.18 [3H, Me], 1.24 [3H, Me], 1.42 [6H, Me], 1.64 (3H, Me), 1.68 (6H, Me), 2.70 [m, CH₂P₂]; $\delta(\text{P})$ 3.66 [1P, PCo], 3.28 [2P, PCo], –31.19 [1P, PCu]. FAB-MS: *m/z* 1195, calcd for $\text{Co}_4\text{Cu}_3(\text{CO})_8(\text{dmpm})_4^+$ 1195, with excellent agreement between observed and calculated isotope patterns. Accurate mass: found 1194.708, calcd 1194.715.

Solution FTIR Studies of the Equilibrium of 1 and 2. FTIR spectra were obtained by using a Bruker IFS 85 spectrophotometer using CaF₂ IR cells cooled by a CTI-Cryogenics Model 22 cryocooler and 350R compressor system with a Lake Shore Cryotronics DRC 80C temperature controller and DT500 DRC silicon diode sensor. The solvent was CH₂Cl₂. In a typical experiment, a solution of $[\text{Co}_2(\text{CO})_4(\mu\text{-dmpm})_2]$ (5.0 mg) in CH₂Cl₂ (1.0 mL) in the IR cell was cooled to 190 K and allowed to equilibrate before recording the spectrum. The sample was then

warmed by 5 K and the procedure repeated. In this way spectra were finally obtained at 5 K intervals between 190 and 300 K. The procedure was repeated using pure solvent, and spectral subtraction then gave the absolute spectra for the 1a/2a mixture at each temperature. The limiting spectra of each isomer were obtained by extrapolation of plots of $\exp(-1/T)$ vs absorbance. The spectrum of the terminal isomer was easily generated, since it should have no absorbance in the bridging carbonyl region at ca. 1700 cm^{-1} . Now that the extinction coefficients for each isomer were known, the equilibrium constant at each temperature was calculated. As a check that the extinction coefficients are not temperature-dependent, values of the equilibrium constant were calculated using absorbance values from at least two different wavelengths; there was excellent agreement. FTIR data in CH₂Cl₂ [$\nu(\text{CO})$, cm^{-1}]: 1a, 1945, 1916, 1735 (sh), 1716; 2a, 1953, 1920, 1893; 1b, 1951, 1924, 1765 (sh), 1753; 2b, 1972, 1953, 1921.

Solution Magnetic Moment Studies of 1a/2a. A sample of $[\text{Co}_2(\text{CO})_4(\mu\text{-dmpm})_2]$ (6.1 mg, 0.01 mmol) was dissolved in CD₂Cl₂ (0.5 mL) containing 5% CH₂Cl₂ and 5% TMS in a 5-mm NMR tube. A 3-mm sealed capillary containing 5% CH₂Cl₂ and

Table VII. Summary of X-ray Structure Determinations

	6	8
formula	C ₁₈ H ₂₈ Co ₄ O ₈ P ₄	C ₂₈ H ₅₆ BCo ₄ Cu ₃ F ₄ P ₈ O ₈
fw	732.04	1281.72
cryst syst, space group	orthorhombic, P2 ₁ 2 ₁ 2 ₁	monoclinic, P2 ₁ /c
cell dimens		
a, Å	14.953(2)	10.767(2)
b, Å	11.386(1)	20.092(2)
c, Å	16.836(1)	22.370(3)
β, deg		92.13(1)
V, Å ³ ; Z	2866.4(6); 4	4836(2); 4
calcd (obsd) density, g cm ⁻³	1.696	1.76 (1.78(5))
λ(Mo Kα), Å; μ(Mo Kα), cm ⁻¹	0.710 69; 25.30	0.710 73; 28.4
R(F _o), R _w (F _o ²) ^a	0.038, 0.051	0.076, 0.066

$$^a R = \sum |F_o| - |F_c| / |F_o|; R_w = [\sum w(|F_o| - |F_c|)^2 / \sum w|F_o|^2]^{1/2}, w = 1/\sigma^2(|F_o|).$$

5% TMS in CD₂Cl₂ was inserted as inner reference, and the cap was closed. ¹H NMR measurements were then recorded from 298 to 183 K. At the end of the experiment the inner capillary was removed and another spectrum was recorded at 298 K.

X-ray Structure Determinations. [Co₄(CO)₈(μ-Me₂PCH₂PMe₂)₂] (6). Purple-black crystals of 6 used in this analysis were grown from a CH₂Cl₂/pentane mixture. All X-ray crystallographic measurements were made with a monocrystal of dimensions ~0.40 × 0.40 × 0.50 mm, graphite-monochromated Mo Kα radiation, and an Enraf-Nonius CAD4 diffractometer.

The unit cell dimensions (Table VII) were determined by a least-squares treatment of diffractometric angles of 25 reflections. The intensity data were measured by θ/2θ scans of (0.80 + 0.35 tan θ)° in θ, and the scan speeds were adjusted to give σ(I)/I ≤ 0.03 subject to a time limit of 60 s. Two standard reflections, remeasured every 2 h throughout data collection, showed no significant variation in intensity. Integrated intensities of all reflections, derived in the usual manner (q = 0.03),⁴⁸ were corrected for Lorentz, polarization, and absorption effects. The last correction, made by an empirical method,⁴⁴ led to transmission factors on F of 0.70–1.23. Of 6773 reflections measured, 1078 were symmetry-related, and their structure amplitudes were averaged to give 539 unique ones and an R(internal) value of 0.030. Only unique reflections with I ≥ 2.5σ(I), of which there were 4769, were used in the structure analysis.

The positions of the cobalt atoms were determined from a Patterson function and those of the remaining non-hydrogen atoms from the subsequent Fourier difference syntheses. All non-hydrogen atoms were allowed anisotropic displacement parameters. The structural model did not include hydrogen atoms but was assigned a polarity parameter, η.⁴⁵ The structure was refined by full-matrix least squares. All calculations were performed using the GX program package.⁴⁶ The neutral-atom scattering factors and anomalous dispersion corrections were taken from ref 47.

[Co₄Cu₃(CO)₈(μ-Me₂PCH₂PMe₂)₄][BF₄] (8). A black crystal, with dimensions 0.15 × 0.12 × 0.34 mm, was mounted in a glass

capillary tube. The density was determined by the neutral buoyancy method. The data collection was carried out by using an Enraf-Nonius CAD4F diffractometer with graphite-monochromated Mo Kα radiation.⁴⁸ Cell constants and an orientation matrix were determined by using the angular settings for 19 high-angle reflections with 24.4 < 2θ < 29.9°. Intensity data were recorded at variable scan speeds chosen to optimize counting statistics within a maximum time per data point of 60 s; background estimates were made by extending the scan by 25% on either side. Standard reflections were monitored every 180 min of X-ray exposure time and showed a random decay of 3% over the total time period of 130 h. Corrections were made for Lorentz, monochromator, and crystal polarization and background radiation effects using the structure determination package⁴⁹ running on a PDP11/23+ computer. An empirical absorption correction was applied.⁵⁰ Scattering factors were from ref 47.

The positions of the Co, Cu, and P atoms were determined using SHELXS-86 running on a SUN 3/50 workstation⁵¹ and all remaining non-hydrogen atoms by subsequent difference Fourier syntheses. Refinement was by full-matrix, least-squares techniques on F using SHELX-76 software.⁵² The Cu, Co, and P atoms were assigned anisotropic thermal parameters. The BF₄⁻ anion was disordered; the geometry was constrained to be regular tetrahedral with B-F = 1.37 Å, and the site occupancies were refined to 70, 20, and 10%. A common isotropic thermal parameter was used for the F atoms in each disorder component of the anion and was refined in the least-squares cycles. Hydrogen atoms were included in idealized positions; a common isotropic temperature factor was assigned to all H atoms and refined. In all, 6699 unique data were observed and refinement was based on 3093 reflections with I ≥ 2.5σ(I) and 295 variables. The crystal data and experimental conditions are given in Table VII. Tables of H atom parameters, anisotropic thermal parameters, root-mean-square amplitudes of vibration, weighted least-squares planes, and torsion angles have been deposited as supplementary material.

Acknowledgment. We thank NATO for a travel grant and Drs. D. J. Elliot, D. G. Holah, and A. N. Hughes for valuable discussions and help. R.J.P. and R.H.H. thank the NSERC (Canada) for financial support.

Supplementary Material Available: Tables S1–S6, giving anisotropic displacement parameters, bond lengths, bond angles, and torsion angles for [Co₄(CO)₈(μ-dmpm)₂] and general displacement parameters and bond distances and angles for [Co₄Cu₃(CO)₈(μ-dmpm)₄][BF₄] (16 pages). Ordering information is given on any current masthead page.

OM920769N

(48) *Enraf-Nonius CAD4F Users Manual*; Enraf-Nonius: Delft, The Netherlands, 1982.

(49) *Enraf-Nonius Structure Determination Package, SDP-PLUS*, Version 3.0, 1985.

(50) North, A. C. T.; Phillips, D. C.; Mathews, F. S. *Acta Crystallogr.* 1968, *A24*, 351.

(51) Sheldrick, G. M. SHELXS-86, Structure Solving Program for Crystal Structure Determination; University of Göttingen: Göttingen, Germany, 1986.

(52) Sheldrick, G. M. SHELX-76, Program for Crystal Structure Determination; University of Cambridge: Cambridge, England, 1976.

(43) Manojlović-Muir, L.; Muir, K. W. *J. Chem. Soc., Dalton Trans.* 1974, 2427.

(44) Walker, N.; Stuart, D. *Acta Crystallogr.* 1983, *A39*, 158.

(45) Rogers, D. *Acta Crystallogr.* 1981, *A37*, 734.

(46) Mallinson, P. R.; Muir, K. W. *J. Appl. Crystallogr.* 1985, *18*, 51.

(47) *International Tables for X-Ray Crystallography*; Kynoch Press: Birmingham, England, 1974; Vol. 4, pp 99, 149.